



## Effects of mammary cancer and chemotherapy on neuroimmunological markers and memory function in a preclinical mouse model

Colleen Netherby-Winslow<sup>a</sup>, Bryan Thompson<sup>a</sup>, Louis Lotta<sup>a</sup>, Mark Gallagher<sup>a</sup>,  
Paige Van Haute<sup>a</sup>, Rachel Yang<sup>a</sup>, Devin Hott<sup>c</sup>, Hamza Hasan<sup>a</sup>, Katherine Bachmann<sup>b</sup>,  
Javier Bautista<sup>a</sup>, Scott Gerber<sup>a</sup>, Deborah A. Cory-Slechta<sup>b</sup>, Michelle Janelsins<sup>a,\*</sup>

<sup>a</sup> Department of Surgery, Division of Supportive Care in Cancer, University of Rochester, Rochester, NY, United States

<sup>b</sup> Department of Neurology, University of Rochester, Rochester, NY, United States

<sup>c</sup> Department of Environmental Medicine, University of Rochester, Rochester, NY, United States

### ARTICLE INFO

#### Keywords:

Mammary cancer  
Chemotherapy  
Cancer-related cognitive decline (CRCDC)  
Memory  
Delayed spatial alternation  
Inflammation  
Neuroinflammation

### ABSTRACT

Treatment modalities for breast cancer, including cyclophosphamide chemotherapy, have been associated with the development of cognitive decline (CRCDC), which is characterized by impairments in memory, concentration, attention, and executive functions. We and others have identified a link between inflammation and decreased cognitive performance in patients with breast cancer receiving chemotherapy. In order to better understand the inflammation-associated molecular changes within the brain related to tumor alone or in combination with chemotherapy, we orthotopically implanted mouse mammary tumors (E0771) into female C57BL/6 mice and administered clinically relevant doses of cyclophosphamide and doxorubicin intravenously at weekly intervals for four weeks. We measured serum cytokines and markers of neuroinflammation at 48 h and up to one month post-treatment and tested memory using a reward-based delayed spatial alternation paradigm. We found that breast tumors and chemotherapy altered systemic inflammation and neuroinflammation. We further found that the presence of tumor and chemotherapy led to a decline in memory over time at the longest delay, when memory was the most taxed, compared to shorter delay times. These findings in a clinically relevant mouse model shed light on possible biomarkers for CRCDC and add to the growing evidence that anti-inflammatory strategies have the potential to mitigate cancer- or treatment-related side effects.

### 1. Introduction

Cancer-related cognitive decline (CRCDC) is a significant clinical problem experienced by up to 75% of patients with breast cancer during chemotherapy, and it remains a significant problem post-treatment in up to 35% of survivors (Janelsins et al., 2017; Magnuson et al., 2021; Hardy et al., 2018). Several studies have associated chemotherapy with decreases in cognitive performance in memory, attention, processing speed, and executive function (Belcher et al., 2022; European et al., 2022; Hardy et al., 2018; Janelsins et al., 2014; Lange et al., 2019). Cognitive impairments have been most severe in patients during and immediately after treatment, but they can persist for several years following treatment (Janelsins et al., 2017). Inflammation has been implicated as a possible mechanism for the development of CRCDC, although the precise etiology remains unknown.

We and others have shown that elevated pro-inflammatory cytokine levels post-chemotherapy are associated with a decline in cognitive performance in patients; however, evidence of cognitive impairment prior to any treatment has also been reported, and CRCDC is not limited to patients receiving chemotherapy (Janelsins et al., 2022; Lange et al., 2019; Wefel et al., 2004). Inflammation is a hallmark of cancer and has been associated with problems in memory in diverse disease settings including aging, infection, and neurodegenerative disorders (Alnefeesi et al., 2020; Hanahan and Weinberg, 2011; Sartori et al., 2012; Simen et al., 2011). Since most preclinical work on the impact of chemotherapy on neurocognitive function has been performed in healthy young animals, there is a pressing need for a clinically relevant animal model to assess the independent contributions of cancer and chemotherapy to the development of CRCDC (Winocur et al., 2018). Such a model would provide a framework to better understand the relative effects of cancer

\* Corresponding author.

E-mail address: [Michelle\\_janelsins@urmc.rochester.edu](mailto:Michelle_janelsins@urmc.rochester.edu) (M. Janelsins).

<https://doi.org/10.1016/j.bbih.2023.100699>

Received 2 October 2023; Received in revised form 26 October 2023; Accepted 28 October 2023

Available online 7 November 2023

2666-3546/© 2023 The Authors. Published by Elsevier Inc. This is an open access article under the CC BY-NC-ND license (<http://creativecommons.org/licenses/by-nc-nd/4.0/>).

and cancer treatment, consider how different treatment schedules may affect progressive or long-term cognitive deficits, and develop interventions that could prevent or alleviate cognitive impairment in patients with cancer. We previously reported that in mice cyclophosphamide chemotherapy alone causes a mild but significant decline in hippocampal-based spatial memory that is sustained over time (Janelsins et al., 2016). The present study aims to assess the interaction of cancer and chemotherapy over time using the same cognitive task.

To that end, we orthotopically implanted mouse mammary tumors in female mice and treated them with either saline or a clinically relevant dose of chemotherapy in order to assess the impact of tumor and/or chemotherapy on systemic inflammation, neural precursors, neuroinflammation, and memory using a delayed spatial alternation paradigm. We performed a comprehensive analysis of serum cytokine and chemokine expression in order to investigate a potential molecular signature associated with CRC. We further assessed the cognitive impact of cancer and chemotherapy using a delayed spatial alternation paradigm (Cory-Slechta et al., 1991), which is similar to clinical assessments of spatial memory that have been employed to assess cognitive status in patients with breast cancer (Fray and Robbins, 1996; Minton and Stone, 2012). In this study, we hypothesized that cancer and chemotherapy each would independently lead to inflammation and memory impairment, and that cognitive impairment would be exacerbated by the combination of cancer and chemotherapy.

## 2. Materials and methods

### 2.1. In vivo murine cancer and chemotherapy models

Female C57BL/6 mice were purchased through Jackson labs, Bar Harbor, Maine, at 23–25 g at 6–10 weeks of age. Upon arrival, all mice were allowed to acclimate to their home cage for two to four weeks prior to initiation of experiments. All animal housing and procedures were performed in compliance with guidelines established by the University Committee on Animal Resources at the University of Rochester.

In order to develop a murine model of breast cancer,  $1.5 \times 10^6$  E0771 mouse mammary adenocarcinoma cells diluted in 100  $\mu$ l HBSS, were orthotopically implanted in the fourth mammary fat pad. The day of the injection of E0771 cells was designated day 0. Primary tumor growth was measured weekly using calipers. Starting on day 10 after tumor implantation, 200 mg/kg cyclophosphamide and 10 mg/kg doxorubicin were administered intravenously (IV) at weekly intervals for four weeks. Mice were euthanized at ethical endpoints designated by the University Committee on Animal Resources at University of Rochester. The chemotherapeutic agents were purchased from Sigma Aldrich (St. Louis, MO). Cyclophosphamide (Cat # C-0768) and doxorubicin (Sigma #D1515) were stored according to manufacturer's instructions until use, at which time they were diluted in sterile water, then brought up to the proper concentration using sterile saline. Dose translation calculations were performed as described (Reagan-Shaw et al., 2008).

Each experiment included four groups: 1) a E0771 cancer only group, 2) a chemotherapy only group, 3) a cancer + chemotherapy group, and 4) a saline only control. For inflammation studies,  $n = 4$  per group was used ( $N = 16$  total). For immunohistochemistry,  $n = 4$  per group; in order to increase the number of images for quantification, we replicated this cohort to include eight total per group for analyses ( $N = 32$ ). For behavioral studies, detailed below, we included five mice per group ( $N = 20$  total).

### 2.2. Cytokine and chemokine/receptor quantification

We measured cytokines and chemokines in mouse serum according to standard operating procedures per manufacturer's protocol. Serum was stored at  $-80$  °C, and all samples were analyzed on a Luminex Magpix (Luminex corp., Austin, TX) in the Cancer Control and

Psychoneuroimmunology Lab (CCPL). A median of 50 beaded reactions per well was used to determine the concentration of cytokine for each replicate. Customized Milliplex xMAP high sensitivity cytokine and cytokine receptor immunoassays kits were used. All samples were run within the same kit batch.

### 2.3. Immunohistochemistry (IHC)

We labeled proliferating cells with Brd-U by injecting the mouse with a 50 mg/kg concentration of Brd-U, using a 5 mg/mL stock four times, once every 2 h, the day before perfusion.

All mice were anesthetized with ketamine hydrochloride (Ketalar, Par Pharmaceuticals 100 mg/kg body weight) and xylazine (AnaSed, Akorn Animal Health; 20 mg/kg body weight) and then perfused transcardially with 10 mL of sterile saline with heparin followed by 50 mL of 4% paraformaldehyde in 0.1 M PB. The brains were isolated, post-fixed overnight in 4% paraformaldehyde in 0.1 M PB and transferred to a solution of 30% sucrose with 0.01% sodium azide in PBS for five days prior to coronal sectioning at 50  $\mu$ m or 30  $\mu$ m on a freezing Microtome (Thermo Scientific Microm HM 430), and stored in cryoprotectant at  $-20$  °C prior to immunohistochemical analysis. Immunohistochemistry was performed on free-floating brain sections. BrdU staining was as follows: sections were washed in six changes of 0.1 M phosphate buffered saline (PBS) at pH 7.4 for 10 min each to remove cryoprotectant, followed by permeabilization in 0.3% Triton X-100 (Sigma Aldrich, St. Louis, MO) in PBS for 10 min. All incubation steps were done with mild rotation. Tissue sections were then rinsed in 3% hydrogen peroxide (Sigma Aldrich, St. Louis, MO) in PBS for 30 min to quench endogenous peroxidases. Sections were incubated in 2 N hydrochloric acid (HCl) for 60 min to denature DNA into single strands which allowed the BrdU antibody to bind. Following HCl incubation, tissue sections were rinsed four times for 10 min each in 0.3% PBS-Triton X-100. Tissue sections were incubated for 1 h at room temperature in 10% normal goat serum followed by overnight incubation at 4 °C in a primary antibody solution containing goat anti-BrdU (1:800, Bio Rad) in 0.3% PBS-Triton X-100 with 1% normal goat serum. Following incubation in the primary antibody solution, sections were washed three times for 10 min each at room temperature to remove the unbound primary antibody. Sections were then moved to a secondary antibody solution containing biotinylated goat anti-rat IgG (1:1000, Vector Laboratories, Burlingame, CA) in 0.3% PBS-Triton X-100 and 1% normal goat serum for 1 h at room temperature. Excess secondary antibody was removed with three washes of 0.3% PBS-Triton X-100 for 10 min each. Sections were then incubated in an avidin-biotin-horseradish peroxidase solution (Vector Laboratories, Burlingame, CA) for 1 h at room temperature. Sections were then washed in three rinses of phosphate buffer (PB) for 10 min each and then incubated in a 3, 3'-diaminobenzidine (DAB) fast-tab solution (Sigma Aldrich, St. Louis, MO) for 5 min. Sections were rinsed in PB and mounted onto Superfrost Plus slides (VWR, West Chester, PA), dried, and cover slipped with Permount Mounting Medium (Toluene 55.15%, Beta-Pinene Polymer 44.85%; Electron Microscopy Sciences), and covered with VWR micro-cover glass.

Positive cells from sections containing the hippocampus were visualized on a Nikon Eclipse Ts2R (Nikon Instruments, Tokyo, Japan). Bright field images were captured at 10X magnification with a Spot Camera and Spot Advanced Software Package (Diagnostic Instruments, Sterling Heights, MI). The other antibodies were prepared in a similar manner, and their concentrations are as follows: anti TNF- $\alpha$ , Novus Biologicals (NBP1- 19,532), primary 1:250, secondary 1:1000 Goat anti-rabbit from Vector Labs, (BA-1000); Anti Iba-1, manufacturer, Wako Chemicals GmbH, Neuss, Germany); stock 50  $\mu$ g/100  $\mu$ l, primary 1:1500, secondary 1:1000, stock concentration 50  $\mu$ g/100  $\mu$ l, primary 1:2500, secondary 1:500; Bromodeoxyuridine (5-bromo-2'-deoxyuridine, Brd-U) Bio Rad, item OBT0030, 1:800 of the stock concentration of 0.5 mg/ml, blocked with goat serum and the goat anti rabbit secondary antibody used at 1:1000.

## 2.4. Cell counting

Cell counting was performed manually with the use of image J multi-points selection tool with two separate technicians blinded to conditions. A total of two to four single plane confocal photomicrographs per area, dentate gyrus, CA1, CA2 and CA3 were acquired on a Nikon Eclipse Ts2R at 10x magnification. Anti-Brd-U and anti Iba-1 positive cells were visualized and recorded. Activated vs ramified microglial cells were counted. Reference images were used to determine if cells were activated or ramified (Norden et al., 2016). Briefly, activated microglia had an increased Iba-1 immunoreactivity and were defined as having larger cell bodies and thicker processes, consistent with a de-ramified morphology. All imaging parameters were the same for each image. Single plane confocal images were used, and cell numbers were manually counted in the granule cell layer of the dentate gyrus (DG) bilaterally using the Image J multi-points selection tool.

## 2.5. Behavioral testing

### 2.5.1. Delayed spatial alternation

Behavioral testing was adapted from a standard delayed alternation protocol developed by Cory-Slechta et al. (1991) and described previously (Janelsins et al., 2016). All groups underwent behavioral assessments (Monday – Friday), except on days they received either chemotherapy or tumor injections.

Briefly, mice were placed in open field operant chambers which contained two levers, each below a light emitting diode, which flanked a pellet trough. During the auto-shaping period, food rewards were dispensed at variable intervals for 20 min, with any lever pressing producing an additional food reward; subsequent to the 20 min, rewards

required a correct lever press. Sessions were terminated after the delivery of 50 food rewards. Following auto-shaping, mice were trained to alternate which of two levers was pressed, with the light above a lever illuminating the “correct” lever to be pressed after a constant delay interval. Following this training, the delayed alternation program was applied, where no lights signaled which was the current correct lever, such that mice were required to remember which lever they had pressed previously and press the alternate lever. Memory was tested using delay values between lever pressing opportunities of 1.5, 3, 6.1, 12.4 and 25 s, with these values presented randomly over the course of 48 sessions (50 reinforcers per session). Testing began four weeks before the initiation of chemotherapy and lasted through 12 weeks post-chemotherapy. Sessions were 30 min in duration and carried out five days per week (M-F), except for days that involved chemotherapy injections or locomotor sessions, for a total of 48 sessions.

### 2.5.2. Locomotor activity

To assess any treatment-related motor deficits that might affect performance on delayed spatial alternation testing, locomotor activity was assessed in photobeam chambers as previously described (Sobolewski et al., 2014). Briefly, spontaneous locomotor activity was measured in chambers equipped with 48-channel infrared photobeams (Med Associates Inc., St. Albans, Vermont). Photobeam breaks were recorded every 5 min for an hour to assess horizontal, vertical, and ambulatory movements.

## 2.6. Statistical analysis

SAS and Graphpad Prism was used for all statistical analyses.

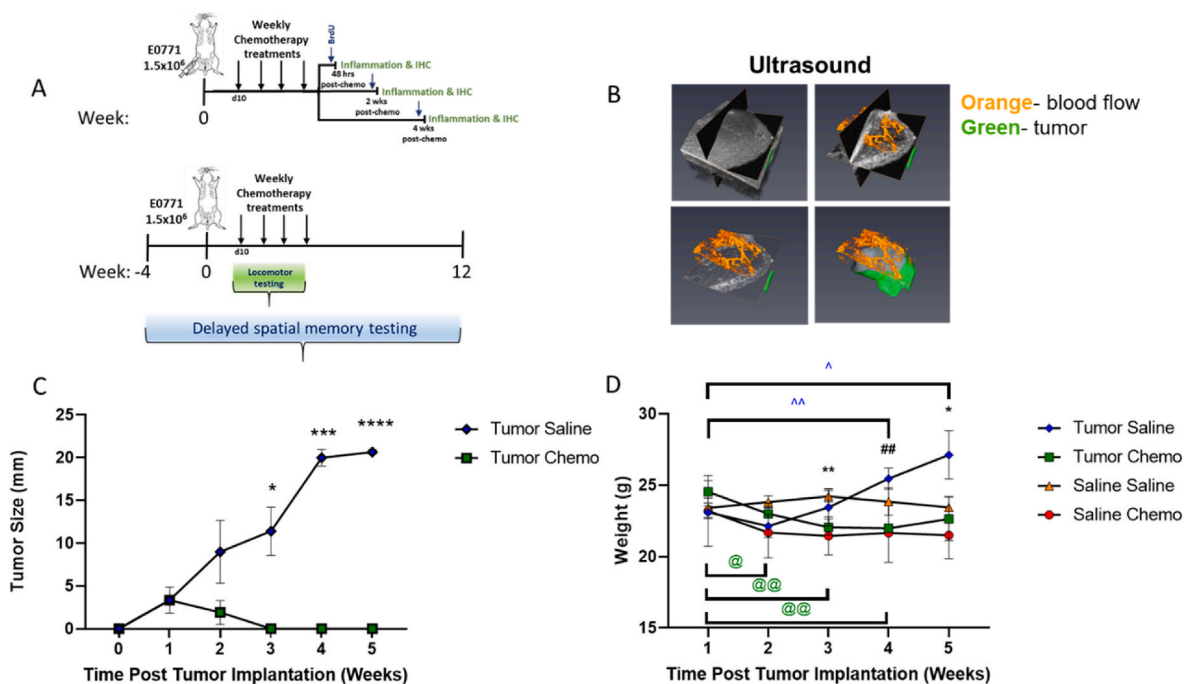


**Fig. 1. Tumor implantation and chemotherapeutic treatment paradigm.** A) Schematic of cancer chemotherapy regimen. Briefly, C57BL/6 mice were randomly divided into four treatment groups ( $n = 4/\text{group}$ ): saline + saline control (S/S), saline + chemotherapy (S/C), tumor + saline (T/S), and tumor + chemotherapy (T/C). The tumor-bearing mice were injected orthotopically implanted with  $1.5 \times 10^6$  of murine mammary gland tumor cell line (E0771) at the fourth mammary fat pad. All mice were tested on a delayed spatial alternation task to assess spatial memory before, during, and following all treatments. Locomotor testing was started at day 10 post tumor implantation and continued weekly for four weeks. B) Tumor size and location via ultrasound depicting blood flow (orange) and tumor (green) at 15 days post injection of  $1.5 \times 10^6$  E0771 murine mammary gland tumor cells in the 4th mammary fat pad. C) Tumor growth was analyzed by two-way ANOVA with Sidák's multiple comparisons test ( $* < 0.05$ ,  $*** < 0.001$ ,  $**** < 0.0001$ ). D) Mice were weighed weekly following tumor implantation and analyzed with mixed-effects analysis, with Tukey's multiple comparisons test ( $** < 0.01$ , S/S vs. T/C;  $## < 0.01$ , T/S vs. T/C;  $* < 0.05$ , S/C vs. T/S). Unpaired T test with Welch's correction was used to compare weights within group to starting weight ( $@ < 0.05$ , T/C week 1 vs. week 2;  $@@ < 0.01$ , T/C week 1 vs. week 3/4;  $< 0.05$ , T/S week 1 vs. week 5;  $< 0.01$ , T/S week 1 vs. week 4). Data representative of two independent experiments.

### 2.6.1. Molecular analyses

In Figs. 1–5, two-way ANOVA with Šídák's multiple comparisons test was used to compare groups. Welch's *t*-test was used to compare within group weights to starting weight (Fig. 1) and to compare cytokine concentrations (Fig. 2) to the S/S control. The significance level was set at an  $\alpha = 0.05$ . Trends are also noted as applicable.

### 2.6.2. Delayed spatial alternation

The experimental design consisted of five factors: Tumor at two levels (Tumor/Saline), Chemo at two levels (Chemo/Saline), Delay Time at five levels (1.5, 3.0, 6.10, 12.40 and 25 s), weeks (11 weeks), and mice (five per Tumor by Saline combination for a total of 20 mice as experimental units). The initial response was the average percentage of times the mouse responded to tasks correctly, and the average is for trials over three to five days. The final measure analyzed as the response was the natural log ratio of average percent correct for a particular week to the average percent correct at Baseline (Log (Ratio)). Higher levels of this measure correspond with better cognition performance. The data were plotted over time for the four treatment combinations (Tumor/Chemo levels) to see the trajectory.

The Log (Ratio) measure was modeled as the response with Tumor, Chemo, and Delay Time treated as fixed effects and weeks and mouse as random effects. A square term for time (weeks) was also incorporated in the model to account for curvature in the data. The Restricted Maximum Likelihood (REML) estimation method was used with an Unstructured Covariance matrix. The Kenward-Roger method was used for estimation of the fixed effects. Verification of the modeling assumptions was also tested.

### 2.6.3. Locomotor function

The average velocity measure was used to assess locomotor function. This response measure was also modeled as a mixed effects model with the same estimation methods mentioned above (REML, Unstructured Covariance Matrix, Kenward-Roger). Tumor and Chemo were treated as fixed effects. A fixed variable Day corresponding to when chemotherapy was applied (Pre-treatment, Mid-treatment and Post-treatment) was also included. A time variable which consisted of 12 5-min intervals was included as a random variable as well as the mouse variable.

## 3. Results

### 3.1. Developing a clinically relevant mouse model for CRCDD to study tumor and treatment responses

An overview of the study paradigm is shown in Fig. 1A. In order to develop a clinically relevant model of CRCDD, we orthotopically implanted E0771 tumors (or saline control) in the fourth mammary fat pad of C57BL/6 mice (as detailed in the methods) and treated with saline alone or with a clinically relevant breast cancer chemotherapy regimen of weekly cyclophosphamide and doxorubicin delivered IV to recapitulate treatment in a neoadjuvant setting. Four treatment groups were used in all experiments: non-tumor bearing mice treated with saline alone (S/S); E0771 tumor-bearing mice treated with saline alone (T/S); non-tumor-bearing mice treated with chemotherapy (S/C); E0771-tumor-bearing mice treated with chemotherapy (T/C). We then assessed systemic serum cytokines by Luminex analysis and IHC for markers of inflammation in the hippocampus, a brain region associated with memory function. We further assessed the cognitive impact of a clinically relevant course of chemotherapy in mice bearing breast tumors using a delayed spatial alternation task. Tumor establishment in the mammary fat pad was confirmed via ultrasound (Fig. 1B). We observed a complete regression of tumors in chemotherapy-treated mice by four weeks post-tumor implantation (Fig. 1C); these tumors did not regrow during the period of analysis. When compared to baseline, chemotherapy alone did not result in significant weight loss (Fig. 1D). However, tumor-bearing mice treated with chemotherapy showed a significant reduction in weight from two to four weeks after chemotherapy was initiated, that partially resolved by the end of treatment (Fig. 1D). Tumor-bearing mice treated only with saline gained weight over the course of treatment compared to baseline and were significantly heavier than non-tumor-bearing mice treated with chemotherapy at five weeks post tumor implantation (Fig. 1D).

### 3.2. Tumor and chemotherapy are associated with changes in systemic inflammation

We found significant changes in the expression of six cytokines in the serum at various timepoints compared among groups and to the saline only control (S/S) (Fig. 2). Tumor alone (T/S) was associated with an early increase in TNF $\alpha$  expression (Fig. 2A,  $p < 0.05$ ). We observed a

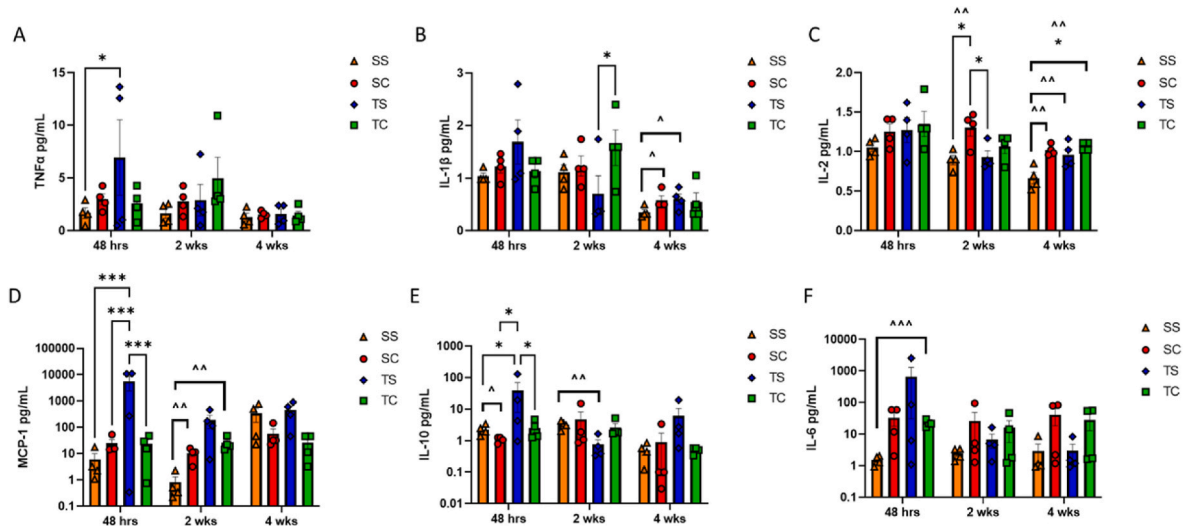


**Fig. 2. Systemic inflammation post-chemotherapy.** Cohorts of mice were euthanized at 48 h, 2 weeks, and 4 weeks post-chemotherapy administration, and serum was analyzed by Luminex for expression of A) TNF $\alpha$ , B) IL-1 $\beta$ , C) IL-2, D) MCP-1, and E) IL-10. Data were analyzed with two-way ANOVA with Tukey's multiple comparisons test (\* $<0.05$  \*\*\* $p < 0.001$ ) as well as with Unpaired T test with Welches correction, with all groups compared to S/S control ( $p < 0.1$ ,  $\bar{p} < 0.05$ ,  $\bar{p} < 0.01$ ).



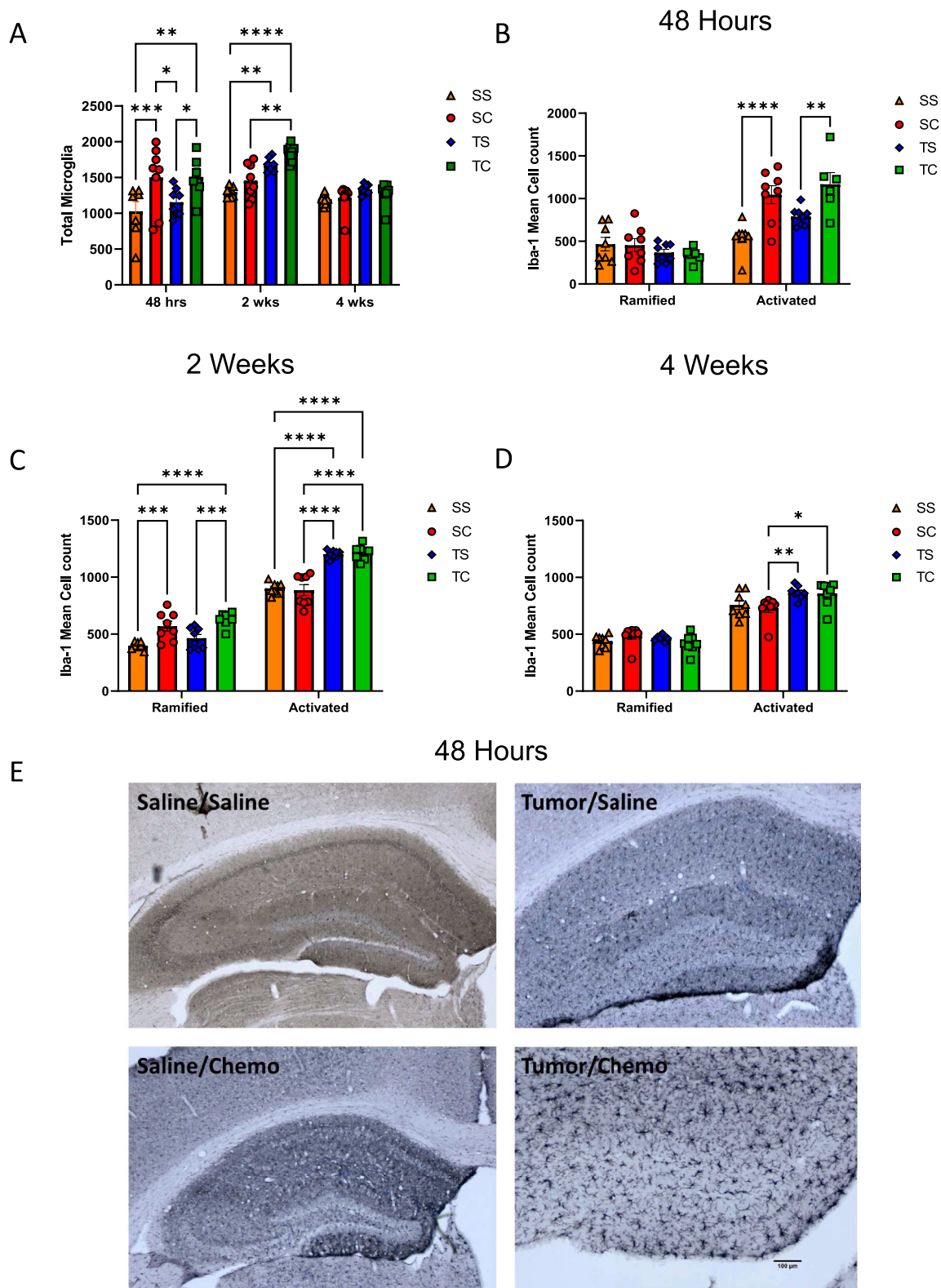


**Fig. 3. Hippocampal neuroinflammation following tumor implantation and chemotherapy.** Cohorts of mice were euthanized and trans-cardially perfused. Fixed brains were stained with Iba-1, and A) total microglial as well as ramified (resting) and activated microglia were quantified in the hippocampus and analyzed with two-way ANOVA with Tukey's multiple comparisons test ( $* < 0.05$ ,  $** < 0.01$ ,  $**** < 0.0001$ ) at B) 48 h, C) 2 weeks, and D) 4 weeks post-chemotherapy administration. E) Representative images of groups at 48 h post-chemotherapy at 4x magnification. Data are representative of two independent experiments.

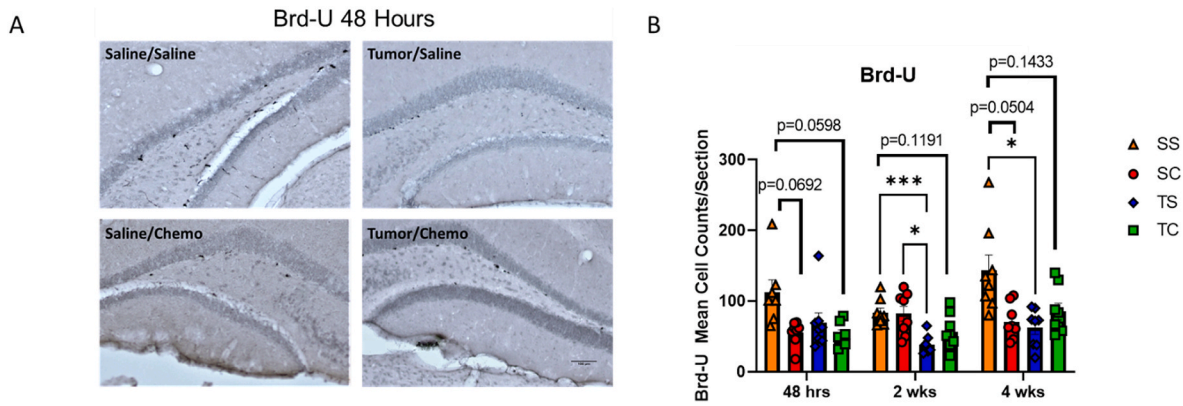


**Fig. 4. Decreased neuronal birthing following tumor implantation and chemotherapy.** Brd-U was administered 24 h prior to mice being euthanized 48 h, 2 weeks, and 4 weeks post-chemotherapy administration and trans-cardial perfusion. Fixed brains were stained for A) Brd-U. Representative images are from the 48 h time point at 10X magnification. B) Quantification of Brd-U and Mixed-effects analysis with Tukey’s multiple comparison test (\* $p < 0.05$ , \*\*\* $p < 0.001$ ). Trends with  $p < 0.2$  are indicated on graph. Data are representative of two independent experiments.

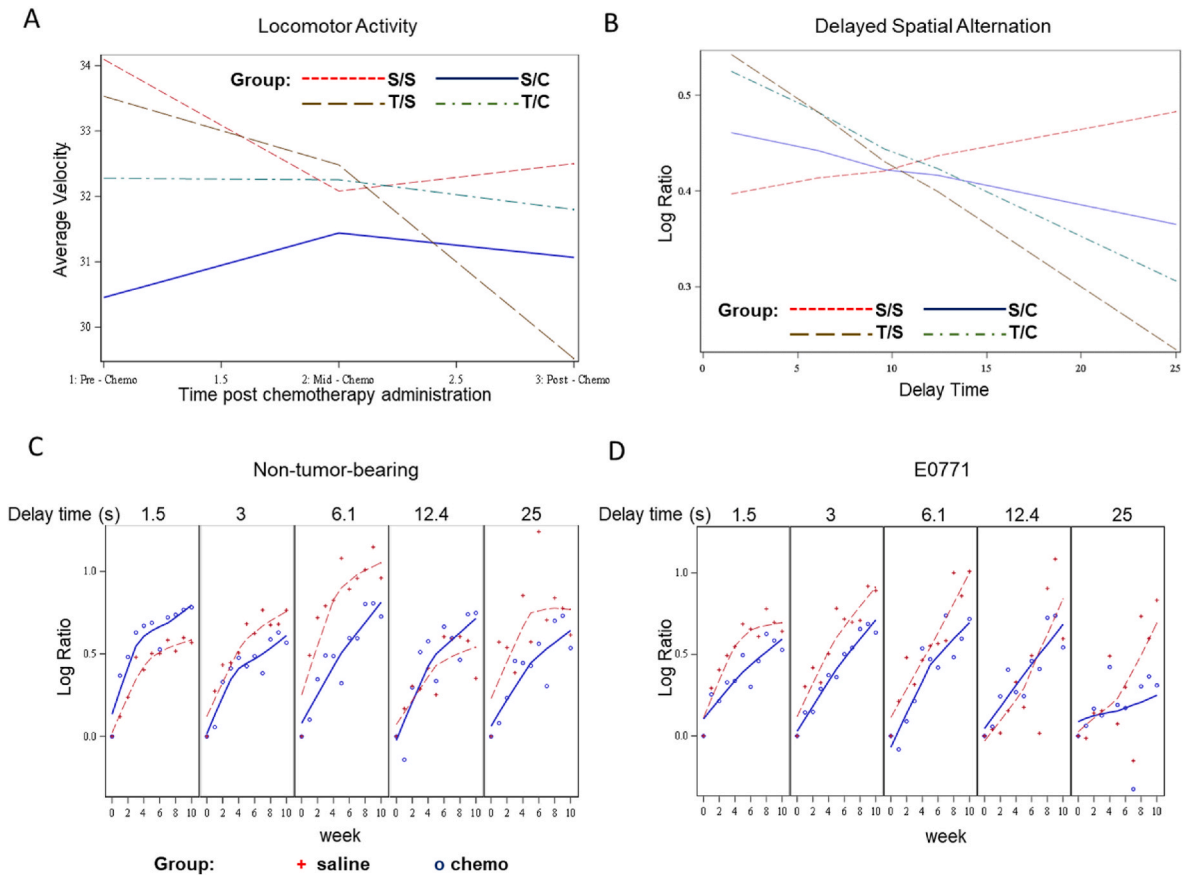


**Fig. 5. The presence of tumor and chemotherapy impact memory function.** A) Mixed model analysis of the interaction between tumor, chemotherapy, and time on locomotor activity. B) Longitudinal mixed model analyses assessed the main effect and interactions of group, time (weeks from baseline), and delay time on percent correct (normalized to baseline) ( $n = 5$  mice/group). C) Interaction of delay time, chemotherapy, and time in non-tumor-bearing mice. D) Interaction of delay time, chemotherapy, and time in E0771-bearing mice.

transient increase in pro-inflammatory IL-1 $\beta$  by two weeks post-chemotherapy in tumor-bearing mice receiving chemotherapy (T/C) compared to tumor-bearing mice treated only with saline (T/S) ( $p < 0.05$ ); this increase was no longer apparent at four weeks (Fig. 2B). When directly compared to the saline only control (S/S), an elevation in IL-1 $\beta$  was evident in the chemotherapy alone (S/C) and tumor alone (T/S) groups (Fig. 2B,  $\leq 0.1$ ) at four weeks post-treatment. Increases in IL-2 emerged later in non-tumor-bearing mice treated with chemotherapy

(S/C) and remained significantly elevated at four weeks post-chemotherapy in tumor-bearing mice treated with chemotherapy (T/C) (Fig. 2C,  $p < 0.05$ ). When directly compared to the saline only control (S/S), we observed persistent elevation of IL-2 in all groups at four weeks post-chemotherapy (Fig. 2C,  $p < 0.05$ ). We found no changes in IL-4 or IL-17 during the treatment course. Interestingly we found that tumor implantation alone (T/S) resulted in a highly significant increase in monocyte chemoattractant protein-1 (MCP-1), a chemokine associated

with infiltration of monocytes and macrophages (Fig. 2D,  $p < 0.001$ ). We observed a concurrent increase in IL-10 in this group (T/S) (Fig. 2E,  $p < 0.05$ ). This elevation in MCP-1 persisted at the two-week timepoint in the chemotherapy alone (S/C) and tumor alone (T/C) groups when compared directly to the saline only group (S/S) ( $p < 0.05$ ); however, IL-10 slightly decreased in the tumor alone group (T/S) by two weeks post-chemotherapy (Fig. 2 D-E,  $\hat{p} < 0.05$ ). An increase in IL-6 was detected only in tumor-bearing mice treated with chemotherapy (T/C) when directly compared to the saline only control at 48 h post-treatment ( $p < 0.01$ ). These data highlight the complex nature of cancer- and chemotherapy-induced inflammation.

### 3.3. Tumor and chemotherapy increases neuroinflammation

In addition to the assessment of systemic inflammation, we also investigated changes within the brain in the same groups at 48 h post-chemotherapy, two weeks post-chemotherapy and one month post-chemotherapy. Total microglia were quantified (Fig. 3A), showing a significant increase in the chemotherapy (SC) and tumor chemotherapy (TC) groups at 48 h. At the two-week timepoint, the tumor plus chemotherapy group (TC) had a significant increase in total microglia. At the four-week timepoint, all groups were equal. A distinction was made between the ramified Iba-1 positive (resting/quiescent microglial cells) and activated Iba-1 positive cells, which can be distinguished morphologically by the presence of an enlarged cell body, amorphous nucleus, and retracted dendrite processes based on reference images. Across all timepoints, the combination of tumor and chemotherapy (S/C, T/S & T/C) increased the level of activated microglial cells in the hippocampus, which indicates an increased level of neuro-inflammation (Fig. 3). At 48 h, chemotherapy alone (S/C) increased the number of activated cells to the same extent as tumor + chemotherapy (T/C) (Fig. 3B, E). By two weeks post-chemotherapy, the tumor-bearing mice with and without chemotherapy (T/S & T/C) exhibited significant microglial activation compared to both control and chemotherapy (S/S & S/C), and a compensatory rebound of resting microglial cells was observed in groups receiving chemotherapy or in the presence of tumor (S/C & T/C) compared to the saline control (S/S) (Fig. 3C). Tumor-bearing mice with and without chemotherapy (T/S & T/C) maintained elevated levels of activated microglial cells at four weeks post-chemotherapy compared to non-tumor bearing mice treated with chemotherapy alone (Fig. 3D).

### 3.4. New neuronal precursor growth is diminished in the presence of tumor and chemotherapy

To assess the status of neuronal precursor cells in the hippocampus, we assayed Brd-U to evaluate proliferating cells in the dentate gyrus of the hippocampus as studied in other neurogenesis studies and studies specific to CRC (Dietrich et al., 2015). Tumor alone (T/S) resulted in a persistent loss of Brd-U staining at two weeks and four weeks (Fig. 4A). Across the three time points, the S/S control maintained a higher level of Brd-U positive cells. At the 48 h and four week time points, a trend towards a reduction in Brd-U in the chemotherapy alone (SC) and tumor plus chemotherapy (TC) groups was seen. The combination of tumor and chemotherapy did not appear to be additive.

### 3.5. Tumor and chemotherapy impact locomotor and memory function

We further set up four separate cohorts of mice to investigate the longitudinal impact of chemotherapy alone or in the presence of tumor-induced inflammation on locomotor function as well as cognitive function in a delayed spatial alternation memory test. Locomotor activity was measured in units of velocity and assessed in photobeam chambers pre-chemotherapy administration, mid-chemotherapy treatment, and post-chemotherapy to assess the development of treatment-related motor deficits that might also impact performance on cognitive tests.

The predictive model showed that average velocity for the control group (S/S) was maintained over the testing period, with a slight decline over time, as expected. The predicted average velocity for the non-tumor-bearing mice treated with chemotherapy (S/C) slightly increased mid-chemotherapy and was maintained at the post-chemotherapy timepoint. The tumor-bearing mice treated with saline (T/S) showed a significant decline in their predicted average velocity over time ( $p < 0.001$ ) (Fig. 5A), suggesting the presence of the growing tumor affected locomotor function. The predicted average velocity in tumor-bearing mice treated with chemotherapy (T/C) dropped substantially from the pre-chemotherapy to mid-chemotherapy time point but was maintained thereafter, suggesting that chemotherapy ameliorates the locomotor deficit associated with untreated tumor growth. Overall, our analyses revealed significant interactions between tumor, chemotherapy, and time ( $p = 0.0147$ ) (Fig. 5, Table 1A).

We tested memory function in mice using a reward-based delayed spatial alternation paradigm with delay values of 1.5, 3, 6.1, 12.4, and 25 s presented randomly over 48 sessions (50 reinforcers per session). Testing took place starting at four weeks before the initiation of chemotherapy and ran through 12 weeks post-chemotherapy. Despite the locomotor deficits observed, mice from all groups received all 50 rewards at each session (data not shown). Longitudinal mixed model analyses assessed the main effect and interactions of group, time (weeks from baseline), and delay time on percent correct (normalized to baseline) (Fig. 5B, Table 1B). Non-tumor-bearing mice treated with saline (S/S) performed consistently well at all delays, while all other treatment groups performed less well as memory delays increased, with a significant delay time  $\times$  group interaction ( $p < 0.05$ ) (Fig. 5B, Table 1B).

To investigate the impact of chemotherapy and tumor alone, we separate groups out by tumor-bearing mice and those that received chemotherapy or saline alone (i.e. non-tumor bearing mice). In non-tumor bearing mice (S/S & S/C) there is a significant delay time by chemotherapy interaction ( $p = 0.0169$ ), suggesting chemotherapy alone leads to a decline in memory function as delay time increases (Fig. 5C, Table 1C). In tumor-bearing mice (T/S & T/C), there is a significant delay time  $\times$  week interaction, suggesting that memory declines over time as delay time increases in both groups ( $p = 0.0073$ ) (Fig. 5C, Table 1D). Taken together these results suggest that the presence of tumor or chemotherapy results in a decline in memory function over time.

## 4. Discussion

Clinical studies have suggested that longitudinally assessed patterns of cytokines can vary temporally in patients with cancer. We sought to assess changes in cytokines over time in a pre-clinical model of cancer and chemotherapy; we also assessed neuroinflammation and behavioral changes. This study is novel because it assesses neuroinflammation and peripheral inflammation in the same clinically relevant model, beyond acute timepoints, using a rigorous study design. Chemotherapy alone has previously been shown to induce systemic and neuroinflammation in mice. In one study, paclitaxel treatment (30 mg/kg) induced a short-term inflammatory response characterized by increased concentrations of circulating LBP, IL-1 $\beta$ , TNF $\alpha$ , and CXCL1, which largely resolved 72 h after chemotherapy administration (Loman et al., 2019). Additional studies have detected no such increase in inflammatory cytokines after paclitaxel treatment (10 mg/kg) at 2 h to 1 week post-treatment (Ray et al., 2011) suggesting a possible dose effect. We assessed the impact of a clinically relevant course of chemotherapy at both short- and long-term intervals up to one month post-treatment to identify changes in inflammatory patterns at various time points. These data provide an understanding of neuroinflammatory molecular changes due to cancer and chemotherapy and support the use of this pre-clinical model as one that recapitulates features of human CRC and allows disease and treatment to both be considered.

We found that 10 mg/kg of doxorubicin plus 200 mg/kg of



**Table 1**

Interaction tables for locomotor activity and delayed spatial alternation. A) Mixed model interactions for locomotor activity. B) In the second analysis we modeled the natural log of the ratio of percent correct in the delayed spatial memory test for that particular week to the percent correct at the baseline - Log (Ratio). The table shows a three-way interaction between delay time, tumor, and chemotherapy. Highlighted values indicate statistical significance. The model was then run by tumor type: C) no tumor and D) E0771-bearing.

A. Type 3 Tests of Fixed Effects: Locomotor Activity				
Groups	All Groups (SS, SC, TS, TC)			
Effect	Num DF	Den DF	F Value	Pr > F
Tumor	1	15.7	1.12	0.3066
Chemo	1	15.7	0.00	0.9865
Tumor*Chemo	1	15.7	1.40	0.2536
Day	2	660	10.87	<0.0001
Tumor*Day	2	660	13.73	<0.0001
Chemo*Day	2	660	6.06	0.0025
Tumor*Chemo*Day	2	660	4.25	0.0147
Time	1	24.1	100.51	<0.0001
B. Type 3 Tests of Fixed Effects: Delayed Spatial Alternation				
Groups	All Groups (SS, SC, TS, TC)			
Effect	Num DF	Den DF	F Value	Pr > F
Tumor	1	23.8	0.10	0.7553
Chemo	1	20	0.38	0.5461
Delaytime	1	1013	0.01	0.9192
Delaytime*Chemo	1	1014	0.58	0.4455
Delaytime*Tumor*Chemo	2	907	2.95	0.053
Week	1	333	63.72	<0.0001
Delaytime*Week*Chemo	2	1026	5.74	0.0033
Weeksq	1	1028	28.57	<0.0001
Weeksq*Chemo	1	33.2	2.72	0.1087
Delaytime*Weeksq*Tumor	2	1022	4.14	0.0162
C. Type 3 Tests of Fixed Effects: Delayed Spatial Alternation				
Groups	Saline Only (SS, SC)			
Effect	Num DF	Den DF	F Value	Pr > F
Chemo	1	9.02	0.16	0.7001
Delaytime	1	525	0.08	0.7769
Delaytime*Chemo	1	525	5.75	0.0169
Week	1	519	37.53	<0.0001
Delaytime*Week	1	525	0.33	0.5651
Weeksq	1	525	13.59	0.0003
Weeksq*Chemo	1	9.26	0.78	0.4007
Delaytime*Weeksq	1	525	0.50	0.4804
D. Type 3 Tests of Fixed Effects: Delayed Spatial Alternation				
Groups	E0771 Only (TS, TC)			
Effect	Num DF	Den DF	F Value	Pr > F
Chemo	1	12	0.42	0.5309
Delaytime	1	489	0.02	0.8915
Delaytime*Chemo	1	489	1.39	0.2395
Week	1	63	27.44	<0.0001
Delaytime*Week	1	489	7.27	0.0073
Weeksq	1	498	16.88	<0.0001
Weeksq*Chemo	1	33.8	2.75	0.1064
Delaytime*Weeksq	1	189	4.81	0.0288

cyclophosphamide weekly in tumor bearing mice (T/C) did not induce robust, long-term changes in peripheral cytokine response when compared to our tumor only group (T/S) at 4 weeks post chemotherapy. When changes in cytokines were compared across groups, increased inflammation was largely observed at the earlier time points following chemotherapy administration. The effect of chemotherapy was more apparent when we compared groups individually to the saline control (S/S); in these instances, chemotherapy alone was associated with increased TNF $\alpha$ , IL-2, MCP-1, and IL-6 levels at various time points following chemotherapy administration. It is likely that these associations were muted due to the main effect of tumor in our model. Compared to the saline control (S/S), IL-2 remained elevated at four

weeks post chemotherapy administration in mice with tumors or with chemotherapy administration alone. IL-2 has context-dependent pro- and anti-inflammatory capabilities, although low dose IL-2 has been shown to selectively activate T regulatory cells (Tregs) without activating effector T cells which can be pathologic in the brain (Klatzmann and Abbas, 2015). IL-2 could be acting to control chemotherapy- or tumor-induced inflammation, as IL-2 has been shown to stimulate regulatory T cells systemically and in the brain (Alves et al., 2017). In line with our finding of persistent microglial activation in the presence of tumor or chemotherapy, IL-2 administration has also been shown to activate astrocytes, although in these contexts IL-2 was associated with improvements in memory deficits in mouse models of Alzheimer's Disease (Alves et al., 2017). Clinical studies of IL-2 in patients with CRC have shown mixed results, although a positive association with increased IL-2 and improved visual memory was reported six months post-chemotherapy in one study (Lyon et al., 2016).

In our model, we found that tumor alone (T/S) resulted in transient increases in TNF $\alpha$ , MCP-1, and IL-10 at 48 h post-chemotherapy. Additionally, we observed that tumor-bearing mice treated with chemotherapy (T/C) displayed an increase in IL-1 $\beta$  at two weeks post-treatment that resolved by four weeks. Some trends were observed in non-tumor-bearing mice treated with chemotherapy (S/C), but, given the study design, were likely obscured by the main effect of the tumor.

MCP-1 has been implicated in mild cognitive impairment in aging adults (Galimberti et al., 2006) and has been shown to increase during breast cancer chemotherapy, resolving slightly by 24 months post-treatment but remaining elevated (Lyon et al., 2016). MCP-1 mediates inflammation by altering the migration of monocytes and macrophages (Conductier et al., 2010). It has been implicated in blood brain barrier (BBB) breakdown (Yao and Tsirka, 2014) and worsening of mild cognitive impairment in Alzheimer's Disease (Lee et al., 2018). Previous studies have shown that IV injection of MCP-1 is sufficient to cause microglial activation (Chiu et al., 2010). The early increase in circulating MCP-1 in tumor-bearing mice is associated with a sustained increase in activated microglia observed in the brain from 48 h to four weeks. Interestingly, chemotherapy alone also increases the amount of activated microglia in the brain, suggesting a distinct MCP-1-independent mechanism of microglial activation.

We observed an impact of tumor alone and tumor plus chemotherapy on the presence of activated microglia in the brain at two weeks and four weeks post chemotherapy. There was a transient increase in resting microglia observed at two weeks post-chemotherapy in all groups compared to the saline control (S/S), that was not observed at the later time point. Previous studies have reported mixed results on the impact of chemotherapy-induced systemic inflammation on neuroinflammation and microglial activation. Increased microglial activation and inflammatory cytokine gene expression in the brain have been associated with cognitive impairment five days post paclitaxel treatment alone (Grant et al., 2023). In this setting, depletion of microglia prior to chemotherapy administration leads to improved memory performance in a contextual fear-conditioning paradigm (Grant et al., 2023). Our data shows that chemotherapy alone as well as in combination with tumor leads to increased microglial activation at 48 h post-treatment; however, at two weeks post-treatment we did not observe an effect of chemotherapy alone. Because of the nature of our experiments, separate cohorts of mice were euthanized at each time point, and potential cohort effects complicate the interpretation of these data over time. Furthermore, we cannot rule out that we may have identified newly recruited monocytes, versus activation of existing microglia, especially given our findings of increased systemic cytokine expression. A separate study from another group reported that three days post-paclitaxel treatment there was a decrease in Iba-1 reactivity in the periventricular nucleus of the hypothalamus and the dentate gyrus of the hippocampus (Loman et al., 2019), regions where we observed robust increases in activated microglia by 48 h post chemotherapy in non-tumor-bearing and tumor-bearing mice. While paclitaxel and other taxanes promote cell



cycle arrest leading to death by stabilizing microtubules, cyclophosphamide and doxorubicin mainly exert cytotoxic effects by crosslinking or intercalating DNA, respectively, inhibiting protein synthesis. Further, preclinical studies of tumor-associated neuroinflammation have been conducted in the context of inflammation and immune infiltration around metastatic foci (Andreou et al., 2017), which are absent in this model. These dichotomous findings reveal how discrepancies in timing of analyses and different chemotherapeutic agents can complicate interpretation of results; thus, these data should be viewed as hypothesis generating.

IL-10 functions primarily as an immune regulatory cytokine; it has been linked to immune suppression in breast cancer. Some evidence suggests that IL-10 can downregulate MCP-1 expression by stimulating monocytes/macrophages; however, the source of these cytokines, whether tumor- or immune cell-secreted, remains to be determined. In primary cultures of subventricular zone cells, IL-10 has been shown to help maintain neural progenitors in an undifferentiated state, upregulating neural markers NESTIN, Sox1/2, Musashi, Mash1, and NICD. Infusion of IL-10 into the lateral ventricle leads to a reduction in NUMB and DCX expression, which recover two weeks after the completion of IL-10 treatment (Perez-Asensio et al., 2013). The role that IL-10 plays in cognition is also unclear. In one study, which assessed relationships between systemic cytokines and cognitive function over a two-year time-frame in women with breast cancer, IL-10 was found to be associated with better executive functioning and cognitive flexibility, but negatively associated with processing speed (Lyon et al., 2016).

We found that chemotherapy alone and in combination with tumor resulted in a trend towards a reduction in new birthing of neurons, as evidenced by Brd-U staining, acutely at 48 h and at four weeks post-treatment. At the two-week timepoint, we observed a significant reduction in Brd-U in the tumor alone group, that was also apparent at the four-week timepoint. Decreased hippocampal neurogenesis has been shown to impair learning and memory in pre-clinical models (Sekeres et al., 2021). Decreased hippocampal Brd-U and Ki-67 staining has been observed in rats treated with methotrexate, paclitaxel, and doxorubicin and associated with poorer performance on tasks that rely on hippocampal function, such as novel object learning, novel object recognition, Morris water maze, and discrimination learning (Sekeres et al., 2021). Park et al. showed that low intensity exercise could improve hippocampal Brd-U expression and mitochondrial function, and improve performance in a Morris water maze task in mice treated with doxorubicin (Park et al., 2018). This work suggests that exercise could alleviate chemotherapy-induced cognitive dysfunction by protecting the brain from oxidative stress and restoring neuroplasticity. These findings demonstrate the complex interplay between tumor and treatment.

We also observed that tumor alone (T/S) affects locomotor function. Locomotor defects could be a functional physical impairment caused by a growing tumor and/or fatigue, which is also a common side effect of cancer chemotherapy. In the study discussed above, 4T1.2 tumors, but not tumor-conditioned media, affected locomotor activity, supporting the idea that the presence of a tumor and not the resultant inflammation was the cause of the impairment. These data provide further insight into the locomotion effect associated with tumor burden observed in the tumor alone group (T/S). We did not observe significant weight loss in groups with chemotherapy alone, despite the well-known association of cytotoxic chemotherapy with anorexia and weight loss. Tumor-bearing mice treated with chemotherapy (T/C) did lose weight during treatment but began to recover by the end of treatment, likely due to the regression of their tumor growth. Tumor-bearing mice treated only with saline (T/S) progressively gained weight over the course of treatment; the presence of a large tumor likely contributed to this observed weight gain. These findings again serve to underscore the context-specific effects of timing, tumor type, and chemotherapeutic regimen on evaluation of preclinical models.

There is currently no effective way to treat the cognitive impairment experienced by patients with cancer, and a full understanding of the role

inflammation may play in the development or severity of CRCDD is lacking. The delayed spatial alternation paradigm used in our model assesses learning and memory over progressively longer delay intervals, with longer intervals requiring better ‘remembering’. This method has been used in experimental psychology to investigate the impact of lead exposure and aging on memory function (Cory-Slechta et al., 1991) and posited as a method by which to evaluate chemotherapy-related effects on cognition (Weiss, 2010). The delayed spatial alternation paradigm can identify subtle changes in cognitive function over time and is analogous to the delayed spatial alternation used in the Cambridge Neuropsychological Test Automated Battery (CANTAB) and other tests used in clinical research to assess cognitive function in patients with cancer (Capuron et al., 2001). The current study showed results similar to those reported in our previous work on the impact of cyclophosphamide alone on memory performance in mice (Janelsins et al., 2016); however, a significant impact of tumor alone was also observed in the current study. Overall, we found that the interactions between tumor, chemotherapy, and delay time were significant, indicating that tumor and chemotherapy caused a memory deficit at the longest delay values, i.e., when memory is most challenged relative to non-treatment. Additionally, we found that this deficit declines significantly over time. When we evaluated the effects of chemotherapy on non-tumor bearing and tumor bearing mice separately, we found that chemotherapy alone had a significant impact at the longest delay values within a session, similar to our previous findings. In tumor-bearing mice, chemotherapy resulted in a decline in memory performance over time. These findings bolster support for the use of this model in subsequent studies of CRCDD using various treatment agents and schedules.

This is also a viable paradigm to evaluate interventions that could ameliorate the effects of cancer and/or cancer treatment on cognitive impairment. Walker et al. investigated the impact of mammary tumor alone and tumor conditioned media on systemic inflammation as well as locomotor function and memory performance on novel object recognition tests (Walker et al., 2018). At 30 days post-tumor implantation, increased levels of IL-1 $\alpha$ , IL-6, G-CSF, and MIP-1 $\alpha$ , were measured in the plasma. We also observed increased IL-6 in tumor-bearing mice treated with chemotherapy (T/C) compared to saline control (S/S). Further, this group manifested an early (4–15 days post-tumor implantation) decline in memory function in mice bearing 4T1.2 and E0771 mouse mammary tumors, which recovered following treatment with an anti-inflammatory agent. However, the impact of the anti-inflammatory agent, aspirin, on the systemic cytokine levels that were increased in tumor-bearing mice was not reported; thus, the mechanism of how aspirin improved memory function remained unclear and is an area for future study. Novel object recognition tasks reportedly rely on hippocampal and perirhinal cortex function—both areas that have been associated with memory and sensory processing (Broadbent et al., 2010; Kinnavane et al., 2016). Additional studies that use relevant cognitive testing to mechanistically link anti-inflammatory therapies with systemic cytokines and/or brain-region-specific alterations are warranted. Taken together, these results shed light on the mechanism of CRCDD and the link between peripheral inflammation, neuroinflammation, and impaired memory.

## 5. Conclusions

This study adds to the existing CRCDD literature by providing evidence for understanding the independent and combined impact of cancer and chemotherapy in a clinically relevant animal model including multiple time-points up to 1 month post-treatment. We found that this model recapitulates features of CRCDD in patients and that tumor and chemotherapy caused a memory deficit over time.

## Funding sources

This work was supported by the National Institutes of Health, National Cancer Institute DP2CA195765, R01CA231014.

## Contributions

Each author declares substantial contributions through the following:

(1) The conception and design of the study, or acquisition of data, or analysis and interpretation of data, (2) drafting the article or revising it critically for important intellectual content,

Please indicate for each author the author contributions in the text field below. Signatures are not required.

Colleen Netherby-Winslow (1,2), Bryan Thompson (1,2), Lou Lotta (1,2), Mark Gallagher (1), Paige Van Haute (2), Rachel Yang (1,2), Devin Hott (1), Hamza Hasan (1), Katherine Bachmann (1,2), Javier Bautista (1,2), Scott Gerber (1), Deborah A. Cory-Slechta (1), Michelle Janelsins (1,2).

## Approval of the submitted version of the manuscript

Please check this box to confirm that all co-authors have read and approved the version of the manuscript that is submitted. Signatures are not required.

## Declaration of competing interest

The authors declare that they have no known competing financial interests or personal relationships that could have appeared to influence the work reported in this paper.

## Data availability

Data will be made available on request.

## Acknowledgements

We thank the Cancer Control Psychoneuroimmunology Lab (CCPL) for assistance with *in vivo* experiments, and the Human Biophysiology Shared Resource (HBSR) at Wilmot Cancer institute for Luminex profiling, and data analysis. We further thank the Cory-Slechta lab for assistance with behavioral experiments.

## References

- Alnefeesi, Y., Siegel, A., Lui, L.M.W., Teopiz, K.M., Ho, R.C.M., Lee, Y., McIntyre, R.S., 2020. Impact of SARS-CoV-2 infection on cognitive function: a systematic review. *Front. Psychiatr.* 11, 621773 <https://doi.org/10.3389/fpsy.2020.621773>. Retrieved from <https://www.ncbi.nlm.nih.gov/pubmed/33643083>.
- Alves, S., Churlaud, G., Audrain, M., Michaelsen-Preusse, K., Fol, R., Souchet, B., Cartier, N., 2017. Interleukin-2 improves amyloid pathology, synaptic failure and memory in Alzheimer's disease mice. *Brain* 140 (3), 826–842. <https://doi.org/10.1093/brain/aww330>. Retrieved from <https://www.ncbi.nlm.nih.gov/pubmed/28003243>.
- Andreou, K.E., Soto, M.S., Allen, D., Economopoulos, V., de Bernardi, A., Larkin, J.R., Sibson, N.R., 2017. Anti-inflammatory microglia/macrophages as a potential therapeutic target in brain metastasis. *Front. Oncol.* 7, 251. <https://doi.org/10.3389/fonc.2017.00251>. Retrieved from <https://www.ncbi.nlm.nih.gov/pubmed/29164051>.
- Belcher, E.K., Culakova, E., Gilmore, N.J., Hardy, S.J., Kleckner, A.S., Kleckner, I.R., Janelsins, M.C., 2022. Inflammation, attention, and processing speed in patients with breast cancer before and after chemotherapy. *J. Natl. Cancer Inst.* 114 (5), 712–721. <https://doi.org/10.1093/jnci/djac022>. Retrieved from <https://www.ncbi.nlm.nih.gov/pubmed/35134984>.
- Broadbent, N.J., Gaskin, S., Squire, L.R., Clark, R.E., 2010. Object recognition memory and the rodent hippocampus. *Learn. Mem.* 17 (1), 5–11. <https://doi.org/10.1101/lm.1650110>. Retrieved from <https://www.ncbi.nlm.nih.gov/pubmed/20028732>.
- Capuron, L., Ravaut, A., Dantzer, R., 2001. Timing and specificity of the cognitive changes induced by interleukin-2 and interferon-alpha treatments in cancer patients. *Psychosom. Med.* 63 (3), 376–386. <https://doi.org/10.1097/00006842-200105000-00007>. Retrieved from <https://www.ncbi.nlm.nih.gov/pubmed/11382265>.
- Chiu, K., Yeung, S.C., So, K.F., Chang, R.C., 2010. Modulation of morphological changes of microglia and neuroprotection by monocyte chemoattractant protein-1 in experimental glaucoma. *Cell. Mol. Immunol.* 7 (1), 61–68. <https://doi.org/10.1038/cmi.2009.110>. Retrieved from <https://www.ncbi.nlm.nih.gov/pubmed/20081877>.
- Conductier, G., Blondeau, N., Guyon, A., Nahon, J.L., Rovere, C., 2010. The role of monocyte chemoattractant protein MCP1/CCL2 in neuroinflammatory diseases.

- J. Neuroimmunol.* 224 (1–2), 93–100. <https://doi.org/10.1016/j.jneuroim.2010.05.010>. Retrieved from <https://www.ncbi.nlm.nih.gov/pubmed/20681057>.
- Cory-Slechta, D.A., Pokora, M.J., Widzowski, D.V., 1991. Behavioral manifestations of prolonged lead exposure initiated at different stages of the life cycle: II. Delayed spatial alternation. *Neurotoxicology* 12 (4), 761–776. Retrieved from <https://www.ncbi.nlm.nih.gov/pubmed/1795900>.
- Dietrich, J., Prust, M., Kaiser, J., 2015. Chemotherapy, cognitive impairment and hippocampal toxicity. *Neuroscience* 309, 224–232. <https://doi.org/10.1016/j.neuroscience.2015.06.016>. Retrieved from <https://www.ncbi.nlm.nih.gov/pubmed/26086545>.
- European, C., Cognition, C., Sleurs, C., Amidi, A., Wu, L.M., Kiesl, D., Perrier, J., 2022. Cancer-related cognitive impairment in non-CNS cancer patients: targeted review and future action plans in Europe. *Crit. Rev. Oncol. Hematol.* 180, 103859 <https://doi.org/10.1016/j.critrevonc.2022.103859>. Retrieved from <https://www.ncbi.nlm.nih.gov/pubmed/36257539>.
- Fray, P.J., Robbins, T.W., 1996. CANTAB battery: proposed utility in neurotoxicology. *Neurotoxicol. Teratol.* 18 (4), 499–504. [https://doi.org/10.1016/0892-0362\(96\)00027-x](https://doi.org/10.1016/0892-0362(96)00027-x). Retrieved from <https://www.ncbi.nlm.nih.gov/pubmed/8866544>.
- Galimberti, D., Fenoglio, C., Lovati, C., Venturelli, E., Guidi, I., Corra, B., Scarpini, E., 2006. Serum MCP-1 levels are increased in mild cognitive impairment and mild Alzheimer's disease. *Neurobiol. Aging* 27 (12), 1763–1768. <https://doi.org/10.1016/j.neurobiolaging.2005.10.007>. Retrieved from <https://www.ncbi.nlm.nih.gov/pubmed/16307829>.
- Grant, C.V., Sullivan, K.A., Wentworth, K.M., Otto, L.D., Strehle, L.D., Otero, J.J., Pyter, L.M., 2023. Microglia are implicated in the development of paclitaxel chemotherapy-associated cognitive impairment in female mice. *Brain Behav. Immun.* 108, 221–232. <https://doi.org/10.1016/j.bbi.2022.12.004>. Retrieved from <https://www.ncbi.nlm.nih.gov/pubmed/36494047>.
- Hanahan, D., Weinberg, R.A., 2011. Hallmarks of cancer: the next generation. *Cell* 144 (5), 646–674. <https://doi.org/10.1016/j.cell.2011.02.013>. Retrieved from <https://www.ncbi.nlm.nih.gov/pubmed/21376230>.
- Hardy, S.J., Krull, K.R., Wefel, J.S., Janelsins, M., 2018. Cognitive changes in cancer survivors. *American Society of Clinical Oncology Educational Book* 38, 795–806. [https://doi.org/10.1200/edbk\\_201179](https://doi.org/10.1200/edbk_201179). Retrieved from [https://ascopubs.org/doi/abs/10.1200/EDBK\\_201179](https://ascopubs.org/doi/abs/10.1200/EDBK_201179).
- Janelsins, M.C., Heckler, C.E., Peppone, L.J., Kamen, C., Mustian, K.M., Mohile, S.G., Morrow, G.R., 2017. Cognitive complaints in survivors of breast cancer after chemotherapy compared with age-matched controls: an analysis from a nationwide, multicenter, prospective longitudinal study. *J. Clin. Oncol.* 35 (5), 506–514. <https://doi.org/10.1200/JCO.2016.68.5826>. Retrieved from <https://www.ncbi.nlm.nih.gov/pubmed/28029304>.
- Janelsins, M.C., Heckler, C.E., Thompson, B.D., Gross, R.A., Opanashuk, L.A., Cory-Slechta, D.A., 2016. A clinically relevant dose of cyclophosphamide chemotherapy impairs memory performance on the delayed spatial alternation task that is sustained over time as mice age. *Neurotoxicology* 56, 287–293. <https://doi.org/10.1016/j.neuro.2016.06.013>. Retrieved from <https://www.ncbi.nlm.nih.gov/pubmed/27371410>.
- Janelsins, M.C., Kesler, S.R., Ahles, T.A., Morrow, G.R., 2014. Prevalence, mechanisms, and management of cancer-related cognitive impairment. *Int. Rev. Psychiatr.* 26 (1), 102–113. <https://doi.org/10.3109/09540261.2013.864260>. Retrieved from <https://www.ncbi.nlm.nih.gov/pubmed/24716504>.
- Janelsins, M.C., Lei, L., Netherby-Winslow, C., Kleckner, A.S., Kerns, S., Gilmore, N., Culakova, E., 2022. Relationships between cytokines and cognitive function from pre- to post-chemotherapy in patients with breast cancer. *J. Neuroimmunol.* 362, 577769 <https://doi.org/10.1016/j.jneuroim.2021.577769>. Retrieved from <https://www.ncbi.nlm.nih.gov/pubmed/34871864>.
- Kinnavane, L., Amin, E., Olarte-Sanchez, C.M., Aggleton, J.P., 2016. Detecting and discriminating novel objects: the impact of perirhinal cortex disconnection on hippocampal activity patterns. *Hippocampus* 26 (11), 1393–1413. <https://doi.org/10.1002/hipo.22615>. Retrieved from <https://www.ncbi.nlm.nih.gov/pubmed/27398938>.
- Klatzmann, D., Abbas, A.K., 2015. The promise of low-dose interleukin-2 therapy for autoimmune and inflammatory diseases. *Nat. Rev. Immunol.* 15 (5), 283–294. <https://doi.org/10.1038/nri3823>. Retrieved from <https://www.ncbi.nlm.nih.gov/pubmed/25882245>.
- Lange, M., Joly, F., Vardy, J., Ahles, T., Dubois, M., Tron, L., Castel, H., 2019. Cancer-related cognitive impairment: an update on state of the art, detection, and management strategies in cancer survivors. *Ann. Oncol.* 30 (12), 1925–1940. <https://doi.org/10.1093/annonc/mdz410>. Retrieved from <https://www.ncbi.nlm.nih.gov/pubmed/31617564>.
- Lee, W.J., Liao, Y.C., Wang, Y.F., Lin, I.F., Wang, S.J., Fuh, J.L., 2018. Plasma MCP-1 and cognitive decline in patients with Alzheimer's disease and mild cognitive impairment: a two-year follow-up study. *Sci. Rep.* 8 (1), 1280. <https://doi.org/10.1038/s41598-018-19807-y>. Retrieved from <https://www.ncbi.nlm.nih.gov/pubmed/29352259>.
- Loman, B.R., Jordan, K.R., Haynes, B., Bailey, M.T., Pyter, L.M., 2019. Chemotherapy-induced neuroinflammation is associated with disrupted colonic and bacterial homeostasis in female mice. *Sci. Rep.* 9 (1), 16490 <https://doi.org/10.1038/s41598-019-52893-0>. Retrieved from <https://www.ncbi.nlm.nih.gov/pubmed/31712703>.
- Lyon, D.E., Cohen, R., Chen, H., Kelly, D.L., McCain, N.L., Starkweather, A., Jackson-Cook, C.K., 2016. Relationship of systemic cytokine concentrations to cognitive function over two years in women with early stage breast cancer. *J. Neuroimmunol.* 301, 74–82. <https://doi.org/10.1016/j.jneuroim.2016.11.002>. Retrieved from <https://www.ncbi.nlm.nih.gov/pubmed/27890459>.

- Magnuson, A., Ahles, T., Chen, B.T., Mandelblatt, J., Janelins, M.C., 2021. Cognitive function in older adults with cancer: assessment, management, and research opportunities. *J. Clin. Oncol.* 39 (19), 2138–2149. <https://doi.org/10.1200/JCO.21.00239>. Retrieved from. <https://www.ncbi.nlm.nih.gov/pubmed/34043437>.
- Minton, O., Stone, P.C., 2012. A comparison of cognitive function, sleep and activity levels in disease-free breast cancer patients with or without cancer-related fatigue syndrome. *BMJ Support. Palliat. Care* 2 (3), 231–238. <https://doi.org/10.1136/bmjspcare-2011-000172>. Retrieved from. <https://www.ncbi.nlm.nih.gov/pubmed/23585925>.
- Norden, D.M., Trojanowski, P.J., Villanueva, E., Navarro, E., Godbout, J.P., 2016. Sequential activation of microglia and astrocyte cytokine expression precedes increased Iba-1 or GFAP immunoreactivity following systemic immune challenge. *Glia* 64 (2), 300–316. <https://doi.org/10.1002/glia.22930>. Retrieved from. <https://www.ncbi.nlm.nih.gov/pubmed/26470014>.
- Park, H.S., Kim, C.J., Kwak, H.B., No, M.H., Heo, J.W., Kim, T.W., 2018. Physical exercise prevents cognitive impairment by enhancing hippocampal neuroplasticity and mitochondrial function in doxorubicin-induced chemobrain. *Neuropharmacology* 133, 451–461. <https://doi.org/10.1016/j.neuropharm.2018.02.013>. Retrieved from. <https://www.ncbi.nlm.nih.gov/pubmed/29477301>.
- Perez-Asensio, F.J., Perpina, U., Planas, A.M., Pozas, E., 2013. Interleukin-10 regulates progenitor differentiation and modulates neurogenesis in adult brain. *J. Cell Sci.* 126 (Pt 18), 4208–4219. <https://doi.org/10.1242/jcs.127803>. Retrieved from. <https://www.ncbi.nlm.nih.gov/pubmed/23843621>.
- Ray, M.A., Trammell, R.A., Verhulst, S., Ran, S., Toth, L.A., 2011. Development of a mouse model for assessing fatigue during chemotherapy. *Comp. Med.* 61 (2), 119–130. Retrieved from. <https://www.ncbi.nlm.nih.gov/pubmed/21535922>.
- Reagan-Shaw, S., Nihal, M., Ahmad, N., 2008. Dose translation from animal to human studies revisited. *Faseb. J.* 22 (3), 659–661. <https://doi.org/10.1096/fj.07-9574LSF>. Retrieved from. <https://www.ncbi.nlm.nih.gov/pubmed/17942826>.
- Sartori, A.C., Vance, D.E., Slater, L.Z., Crowe, M., 2012. The impact of inflammation on cognitive function in older adults: implications for healthcare practice and research. *J. Neurosci. Nurs.* 44 (4), 206–217. <https://doi.org/10.1097/JNN.0b013e3182527690>. Retrieved from. <https://www.ncbi.nlm.nih.gov/pubmed/22743812>.
- Sekeres, M.J., Bradley-Garcia, M., Martinez-Canabal, A., Winocur, G., 2021. Chemotherapy-induced cognitive impairment and hippocampal neurogenesis: a review of physiological mechanisms and interventions. *Int. J. Mol. Sci.* 22 (23) <https://doi.org/10.3390/ijms222312697>. Retrieved from. <https://www.ncbi.nlm.nih.gov/pubmed/34884513>.
- Simen, A.A., Bordner, K.A., Martin, M.P., Moy, L.A., Barry, L.C., 2011. Cognitive dysfunction with aging and the role of inflammation. *Ther. Adv. Chronic Dis* 2 (3), 175–195. <https://doi.org/10.1177/2040622311399145>. Retrieved from. <https://www.ncbi.nlm.nih.gov/pubmed/23251749>.
- Sobolewski, M., Conrad, K., Allen, J.L., Weston, H., Martin, K., Lawrence, B.P., Cory-Slechta, D.A., 2014. Sex-specific enhanced behavioral toxicity induced by maternal exposure to a mixture of low dose endocrine-disrupting chemicals. *Neurotoxicology* 45, 121–130. <https://doi.org/10.1016/j.neuro.2014.09.008>. Retrieved from. <https://www.ncbi.nlm.nih.gov/pubmed/25454719>.
- Walker, A.K., Chang, A., Ziegler, A.I., Dhillon, H.M., Vardy, J.L., Sloan, E.K., 2018. Low dose aspirin blocks breast cancer-induced cognitive impairment in mice. *PLoS One* 13 (12), e0208593. <https://doi.org/10.1371/journal.pone.0208593>. Retrieved from. <https://www.ncbi.nlm.nih.gov/pubmed/30532184>.
- Wefel, J.S., Lenzi, R., Theriault, R.L., Davis, R.N., Meyers, C.A., 2004. The cognitive sequelae of standard-dose adjuvant chemotherapy in women with breast carcinoma: results of a prospective, randomized, longitudinal trial. *Cancer* 100 (11), 2292–2299. <https://doi.org/10.1002/cncr.20272>. Retrieved from. <https://www.ncbi.nlm.nih.gov/pubmed/15160331>.
- Weiss, B., 2010. Evaluation of multiple neurotoxic outcomes in cancer chemotherapy. *Adv. Exp. Med. Biol.* 678, 96–112. [https://doi.org/10.1007/978-1-4419-6306-2\\_13](https://doi.org/10.1007/978-1-4419-6306-2_13). Retrieved from. <https://www.ncbi.nlm.nih.gov/pubmed/20738011>.
- Winocur, G., Johnston, I., Castel, H., 2018. Chemotherapy and cognition: international cognition and cancer task force recommendations for harmonising preclinical research. *Cancer Treat Rev.* 69, 72–83. <https://doi.org/10.1016/j.ctrv.2018.05.017>. Retrieved from. <https://www.ncbi.nlm.nih.gov/pubmed/29909223>.
- Yao, Y., Tsirka, S.E., 2014. Monocyte chemoattractant protein-1 and the blood-brain barrier. *Cell. Mol. Life Sci.* 71 (4), 683–697. <https://doi.org/10.1007/s00018-013-1459-1>. Retrieved from. <https://www.ncbi.nlm.nih.gov/pubmed/24051980>.